



OPTIMAL PLACEMENT AND ACTIVE VIBRATION CONTROL OF COMPOSITE PLATES INTEGRATED PIEZOELECTRIC SENSOR/ACTUATOR PAIRS

Tran Huu Quoc, Vu Van Tham*, Tran Minh Tu

University of Civil Engineering, 55 Giai Phong Road, Hai Ba Trung District, Ha Noi

*Email: vuthamxd@gmail.com

Received: 1 November 2016; Accepted for publication: 3 January 2018

Abstract. This paper develops a finite element model based on first-order shear deformation theory for optimal placement and active vibration control of laminated composite plates with bonded distributed piezoelectric sensor/actuator pairs. The nine-node isoparametric rectangular element with five degrees of freedom for the mechanical displacements, and two electrical degrees of freedom is used. Genetic algorithm (GA) is applied to maximize the fundamental natural frequencies of plates and the constants feedback control method is used for the vibration control analysis of piezoelectric laminated composite plates. Numerical results showed the accuracy of the presented method against relevant published literatures.

Keywords: composite plate, FEM, active control, optimization, Genetic Algorithm, piezoelectric.

Classification numbers: 5.4.2, 5.4.3, 5.4.5.

1. INTRODUCTION

During the past decade, the application of piezoelectric materials has steadily increased. The piezoelectric elements can be used as automotive sensors, actuators, transducers and active damping devices, etc. Piezoelectric materials show coupling phenomenon between elastic and electric fields, they induce an electric potential/charge when they are deformed, which is called as the direct piezoelectric effect. Conversely, an applied electric field will produce its deformation, which is named the converse piezoelectric effect.

The location of piezoelectric sensor/actuator has significant influence on performance, such as controllability, observability, stability and efficiency of control systems. Hence, the problem of determining the optimal locations of actuators for the active vibration control of flexible structures plays important role in engineering application.

Using the eigenvalues distribution of the energy correlative matrix of control input forces Ning [1] determined optimal number of actuators in active vibration control of structures. Qiu et al. [2] used discrete piezoelectric sensors and actuators to investigate active vibration control of smart flexible cantilever plate. Optimal placement of sensors and actuators is performed based on piezoelectric control equation. Han and Lee [3] used genetic algorithms to find the efficient locations of piezoelectric sensors and actuators in composite plates. Bruant et al. [4] also used a genetic algorithm to optimize the number of sensors and location needed to ensure good

observability. Using modified control matrix and singular value decomposition (MCSVD) approach, Deepak et al. [5] studied the optimal placement of piezoelectric actuators on a thin plate. Ngoc and Thinh [6] used genetic algorithms to determine the efficient locations of piezoelectric actuators in cantilever laminated composite plate.

The aim of present study is to develop a smart nine-noded isoparametric element based on first-order shear deformation theory for optimal placement and active vibration control of laminated composite plates with collocated piezoelectric sensor/actuator pairs. The integer code genetic algorithm (GA) has been utilized to find the optimal locations of the piezoelectric pairs to maximize the natural frequencies of piezoelectric laminated composite plate and a constant feedback control algorithm is used for dynamic response control through a closed loop.

2. PIEZOELECTRIC LAMINATED COMPOSITE FINITE ELEMENT MODELING

2.1. Linear piezoelectric constitutive equations

The constitutive relations for the piezoelectric composite materials of k^{th} layer are given by [7, 8]:

$$\{\sigma^k\} = [\bar{Q}^k] \{\varepsilon^k\} + [e^k] \{E^k\} \quad (1)$$

$$\{D^k\} = \{e^k\}^T \{\varepsilon^k\} + [p^k] \{E^k\} \quad (2)$$

where for k^{th} layer: $\{\sigma^k\} = \{\sigma_x \ \sigma_y \ \sigma_{xy} \ \sigma_{yz} \ \sigma_{xz}\}^T$ is the elastic stress vector; $\{\varepsilon^k\} = \{\varepsilon_x \ \varepsilon_y \ \gamma_{xy} \ \gamma_{yz} \ \gamma_{xz}\}^T$ is the elastic strain vector; $[\bar{Q}^k]$ is the material stiffness matrix; $\{E^k\}$ and $\{D^k\}$ are the electric field and electric displacements vectors; $[p^k]$ and $[e^k]$ are the permittivity coefficient and piezoelectric stress coefficient matrices.

2.2. Displacements and strains based on FSDT

According to the first-order shear deformation theory by [9], the displacement field takes the following form

$$\begin{aligned} u(x, y, z, t) &= u_0(x, y, t) + z\theta_x(x, y, t) \\ v(x, y, z, t) &= v_0(x, y, t) + z\theta_y(x, y, t) \\ w(x, y, z, t) &= w_0(x, y, t) \end{aligned} \quad (3)$$

The compact form of the strain vector at any point (x, y, z) referred to the plate coordinate system can be expressed as

$$\{\bar{\varepsilon}\} = [Z] \{\varepsilon_0\} \quad (4)$$

where

$$\{\bar{\varepsilon}\} = \{\varepsilon_x \ \varepsilon_y \ \gamma_{xy} \ \gamma_{xz} \ \gamma_{yz}\}^T \quad (5)$$

$$[Z] = \begin{bmatrix} 1 & 0 & 0 & 0 & 0 & z & 0 & 0 \\ 0 & 1 & 0 & 0 & 0 & 0 & z & 0 \\ 0 & 0 & 0 & 0 & 1 & 0 & 0 & z \\ 0 & 0 & 0 & 1 & 0 & 0 & 0 & 0 \\ 0 & 0 & 1 & 0 & 0 & 0 & 0 & 0 \end{bmatrix} \quad (6)$$

$$\{\varepsilon_0\} = \left\{ \frac{\partial u_0}{\partial x} \quad \frac{\partial v_0}{\partial y} \quad \frac{\partial u_0}{\partial y} + \frac{\partial v_0}{\partial x} \quad \frac{\partial w_0}{\partial x} + \theta_x \quad \frac{\partial w_0}{\partial y} + \theta_y \quad \theta_{x,x} \quad \theta_{y,y} \quad \theta_{x,y} + \theta_{y,x} \right\} \quad (7)$$

Hooke's law for k^{th} orthotropic layer of laminated composite plate in the local coordinate is written as

$$\begin{Bmatrix} \sigma_1 \\ \sigma_2 \\ \tau_{12} \\ \tau_{13} \\ \tau_{23} \end{Bmatrix}^{(k)} = \begin{bmatrix} Q_{11} & Q_{12} & Q_{16} & 0 & 0 \\ Q_{21} & Q_{22} & Q_{26} & 0 & 0 \\ Q_{61} & Q_{62} & Q_{66} & 0 & 0 \\ 0 & 0 & 0 & Q_{55} & Q_{54} \\ 0 & 0 & 0 & Q_{45} & Q_{44} \end{bmatrix}^{(k)} \begin{Bmatrix} \varepsilon_1 \\ \varepsilon_2 \\ \gamma_{12} \\ \gamma_{13} \\ \gamma_{23} \end{Bmatrix}^{(k)} \quad (8)$$

where the elastic constants Q_{ij} are given by

$$Q_{11} = \frac{E_1}{1 - \nu_{12}\nu_{21}}, \quad Q_{12} = \frac{\nu_{12}E_2}{1 - \nu_{12}\nu_{21}}, \quad Q_{22} = \frac{E_2}{1 - \nu_{12}\nu_{21}}, \quad Q_{66} = G_{12}, \quad Q_{55} = G_{13}, \quad Q_{44} = G_{23} \quad (9)$$

in which E_1, E_2 are Young's modulus in the 1 and 2 directions, respectively; G_{12}, G_{23}, G_{13} are the shear modulus in the 1-2, 2-3 and 3-1 planes, respectively; and ν_{ij} are the Poisson's ratios.

The constitutive relations for the k^{th} orthotropic lamina referred to (x, y, z) global coordinate systems is computed by

$$\begin{Bmatrix} \sigma_x \\ \sigma_y \\ \tau_{xy} \\ \tau_{xz} \\ \tau_{yz} \end{Bmatrix}^{(k)} = \begin{bmatrix} \bar{Q}_{11} & \bar{Q}_{12} & \bar{Q}_{16} & 0 & 0 \\ \bar{Q}_{21} & \bar{Q}_{22} & \bar{Q}_{26} & 0 & 0 \\ \bar{Q}_{61} & \bar{Q}_{62} & \bar{Q}_{66} & 0 & 0 \\ 0 & 0 & 0 & \bar{Q}_{55} & \bar{Q}_{54} \\ 0 & 0 & 0 & \bar{Q}_{45} & \bar{Q}_{44} \end{bmatrix}^{(k)} \begin{Bmatrix} \varepsilon_x \\ \varepsilon_y \\ \gamma_{xy} \\ \gamma_{xz} \\ \gamma_{yz} \end{Bmatrix}^{(k)} \quad (10)$$

where \bar{Q}_{ij} are transformed plane reduced elastic constants of the k^{th} lamina given by [9].

2.3. Isoparametric quadratic element

The nine-noded isoparametric quadratic element is adopted and the interpolation formulas for the spatial coordinates are:

$$x = \sum_{i=1}^9 N_i x_i \quad y = \sum_{i=1}^9 N_i y_i \quad (11)$$

where $N_i(\xi, \eta)$ are the quadratic shape functions.

The generalized displacement vector $\{u\}$ at any point within the element can be written as

$$\{u(\xi, \eta)\} = \sum_{i=1}^n N_i(\xi, \eta) \{u\}_i; \quad n = 9 \quad (12)$$

in which N_i is shape function, $\{u\}_i$ is the nodal generalized displacement vector. From equations (4), (7) and (12), the generalized strain vector $[\bar{\epsilon}]$ are obtained as

$$\{\bar{\epsilon}\} = [Z][B_u]\{u\}_i \quad (13)$$

where

$$[B]_u = [[B_1] \ [B_2] \ \dots \ [B_9]] \quad (14)$$

with

$$[B_i] = \left[[B_i^m] \ [B_i^b] \ [B_i^s] \right]^T \quad (15)$$

$$[B_i^m] = \begin{bmatrix} N_{i,x} & 0 & 0 & 0 & 0 \\ 0 & N_{i,y} & 0 & 0 & 0 \\ N_{i,y} & N_{i,x} & 0 & 0 & 0 \end{bmatrix}; \quad [B_i^b] = \begin{bmatrix} 0 & 0 & 0 & N_{i,x} & 0 \\ 0 & 0 & 0 & 0 & N_{i,y} \\ 0 & 0 & 0 & N_{i,y} & N_{i,x} \end{bmatrix}; \quad [B_i^s] = \begin{bmatrix} 0 & 0 & N_{i,x} & N_i & 0 \\ 0 & 0 & N_{i,y} & 0 & N_i \end{bmatrix} \quad (16)$$

in which $N_{i,x}$, $N_{i,y}$ are the derivatives of the shape functions with respect to x and y respectively ($i = 1, 2, \dots, 9$).

2.4. Electric field-electric potential relations

The electric potential functions are assumed to be varied linearly across the thickness of the piezoelectric actuator/sensor layers. The electric potential vector $\{\phi_i\}$ of the i^{th} element can be determined as

$$\{\phi_i\} = \{\phi^{(1)} \ \phi^{(2)} \ \dots \ \phi^{(N_p)}\}^T \quad (17)$$

where N_p is the number of piezoelectric layers and $\phi^{(k)}$ ($k=1, 2, \dots, N_p$) is the electric potential of the k^{th} piezoelectric layer in the i^{th} element.

The electric field vector $\{E_j\}$ in the j^{th} piezoelectric layer can be expressed as

$$\{E_j\} = \left[0 \ 0 \ -\frac{\phi^{(j)}}{h_j} \right]^T \quad (j=1, 2, \dots, N_p) \quad (18)$$

where h_j is the thickness of j^{th} piezoelectric layer in the i^{th} element.

2.5. Equations of motion

The equations of motion for the laminated composite plate with integrated piezoelectric sensors and actuators can be derived using the Hamilton's principle [7, 10, 8]:

$$\begin{bmatrix} M_{uu} & 0 \\ 0 & 0 \end{bmatrix} \begin{Bmatrix} \ddot{u} \\ \ddot{\phi} \end{Bmatrix} + \begin{bmatrix} K_{uu} & K_{u\phi} \\ K_{\phi u} & K_{\phi\phi} \end{bmatrix} \begin{Bmatrix} u \\ \phi \end{Bmatrix} = \begin{Bmatrix} F \\ Q_c \end{Bmatrix} \quad (19)$$

or in the following form

$$\begin{cases} M_{uu}\ddot{u} + K_{uu}u + K_{u\phi}\phi = F \\ K_{\phi u}u + K_{\phi\phi}\phi = Q_c \end{cases} \quad (20)$$

Substituting the second equation of (20) into the first equation of (20) yields:

$$M_{uu}\ddot{u} + (K_{uu}u + K_{u\phi}K_{\phi\phi}^{-1}K_{\phi u})u = F + K_{u\phi}K_{\phi\phi}^{-1}Q_c \quad (21)$$

here u , ϕ , F and Q_c are the global vectors of displacement, electric potential, applied force and charge, respectively.

The mass matrix:

$$M_{uu} = \int_V \rho [N]^T [N] dV \quad (22)$$

The mechanical stiffness matrix:

$$[K_{uu}] = \int_S [B_u]^T [H] [B_u] dS \quad (23)$$

The mechanical-electrical coupling stiffness matrix:

$$[K_{u\phi}] = \int_S [B_u]^T [\bar{e}] [B_\phi] dS \quad (24)$$

The electrical-mechanical coupling stiffness matrix:

$$[K_{\phi u}] = [K_{u\phi}]^T \quad (25)$$

The piezoelectric permittivity stiffness matrix:

$$[K_{\phi\phi}] = - \int_S [B_\phi]^T [\bar{p}] [B_\phi] dS \quad (26)$$

where $[B_\phi]$ is the strain potential matrix and $[B_u]$ is called the strain-displacement matrix.

For free harmonic vibration of the n^{th} mode, Eq. (19) can be written in the form [7]

$$\begin{aligned} (K_{uu} - \omega_n^2 M_{uu})u + K_{u\phi}\phi &= 0 \\ K_{\phi u}u + K_{\phi\phi}\phi &= 0 \end{aligned} \quad (27)$$

where ω_n is the angular natural frequency corresponding to mode n . By performing the condensation of the electrical potential degrees of freedom we obtain

$$(K^* - \omega_n^2 M_{uu})u = 0 \quad (28)$$

where

$$K^* = K_{uu} - K_{u\phi}K_{\phi\phi}^{-1}K_{\phi u} \quad (29)$$

3. ACTIVE CONTROL BY SENSORS AND ACTUATORS

Consider a laminated piezoelectric composite rectangular plate of sides a and b with thickness h consist n layers as shown in Figure 1. The top layer serves as actuator denoted with subscript "a" and the bottom layer serves as sensor denoted with subscript "s". When the plate

vibrates, electric displacements are induced on the sensor surface. The charges are collected in the thickness direction. Through closed loop control, the charges increase the electric potentials, which are then amplified and converted into the open circuit voltage. Next, the signal is then fed back into the distributed actuator, which causes deformation. The stress resultant induced can actively control the dynamic response of the laminates.

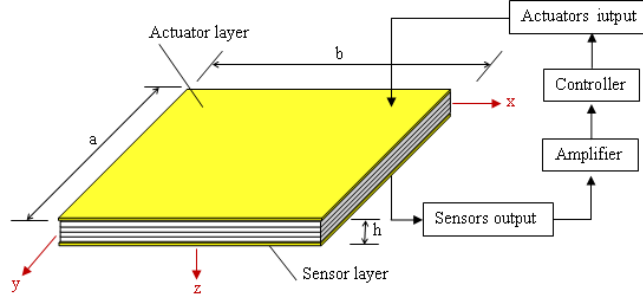


Figure 1. Schematic diagram of a laminate plate with integrated piezoelectric sensors and actuators.

The actuating voltage vector ϕ_a can be written as

$$\phi_a = G_d \phi_s + G_v \dot{\phi}_s \quad (30)$$

in which, the constant gains G_d and G_v of the displacement feedback control and velocity feedback control introduced by [11], and ϕ_s is sensing voltage vector.

Without the external charge Q , the generated potential on the sensor layer can be derived from the second equation of (20) as:

$$\phi_s = [K_{\phi\phi}^{-1}]_s [K_{\phi u}]_s u_s \quad (31)$$

and the induced charge due to the deformation is

$$Q_s = [K_{\phi u}]_s u_s \quad (32)$$

Substitution of the above equation into equation (20) leads to

$$Q_a = [K_{\phi u}]_a u_a - G_d [K_{\phi\phi}]_a [K_{\phi\phi}^{-1}]_s [K_{\phi u}]_s u_s - G_v [K_{\phi\phi}]_a [K_{\phi\phi}^{-1}]_s [K_{\phi u}]_s \dot{u}_s \quad (33)$$

Substituting equations (31) and (33) into equation (21), we get

$$M_{uu} \ddot{u} + C_a \dot{u} + K_{uu}^* u = F \quad (34)$$

where C_a is the active damping matrix in the form

$$C_a = G_v [K_{\phi\phi}]_a [K_{\phi\phi}^{-1}]_s [K_{\phi u}]_s \quad (35)$$

$$K_{uu}^* = [K_{uu}] - G_d [K_{u\phi}]_s [K_{\phi\phi}^{-1}]_s [K_{\phi u}]_s \quad (36)$$

If the structural damping effect is incorporated into equation (34), it can be rewritten as

$$M_{uu} \ddot{u} + (C_a + C_d) \dot{u} + K_{uu}^* u = F \quad (37)$$

where C_d is the Rayleigh damping matrix of the structure, which can be expressed as

$$C_d = \alpha M_{uu} + \beta K_{uu} \quad (38)$$

in which α and β are the Rayleigh damping coefficients.

4. OPTIMAL DESIGN

In this section, the Genetic Algorithm is used to find the optimal placement of fix number of piezoelectric actuators/sensor pairs based on the objective fitness, which is the maximum fundamental natural frequency. The discrete optimal sensor/actuator pair location problem is formulated in the form of a zero-one optimization problem. A zero performs the absence of a sensor/actuator pair and one represents the presence of a sensor/actuator pair on the element. Genetic algorithms are random search techniques derived from principles of natural selection and genetics. The decision parameters are coded as a string of binary bits that corresponds to the chromosome in natural genetics. The objective function value corresponding to the design vector plays the role of fitness in natural genetics. The artificial recombination among the population of strings is based on the fitness and the accumulated knowledge. In every new generation, a new set of strings is created by creation of three kinds of children: Elite, Crossover and Mutation children. In each generation, the best parents are selected based on their fitness values.

The application of GA for the optimization problems can be outlined as :

- The initial population is created randomly. The length of each chromosome will be equal to the number of finite elements in the structure.
- Calculate the fitness value. Genetic operators are applied to reproduce a new set of chromosomes.
- The maximization problem is converted into a minimization problem with fitness $f(x) = -J_{opt}$.
- A constraint of the problem is that the total number of sensor/actuator pairs is equal to a given fixed number.

5. NUMERICAL RESULTS AND DISCUSSIONS

5.1. Free vibration of simply supported square piezoelectric laminate

The first numerical problem is used to validate the developed models.

Free vibration of simply supported square piezoelectric laminates plates with thickness $h = 0.01$ m and side length $a = 50 h$ (Figure 2) is analyzed. The laminate consists of a four-layer Graphite-Epoxy sub-laminate and two PZT-4 outer layers. Each elastic layer has a thickness of $0.2 h$, whereas each piezoelectric layer has thickness of $0.1 h$. The material properties are given in Ref. [12]. In addition, all layers are assumed to have a unit density ($\rho = 1 \text{ kg/m}^3$). The cases of closed-circuit condition and open-circuit condition are considered. Table 1 presented the fundamental natural frequencies of laminated piezoelectric rectangular plate. The results are compared with those reported by [12], in which the spline finite strip method was applied.

It can be seen that the fundamental frequency of the plates in case of closed-circuit is smaller than in case of open-circuit condition. The maximum discrepancy between the results of present study with those of Akhras [12] is 2.55 % (%Error = $100\% \times (\text{Akhras [12]} - \text{Present}) / \text{Present}$). It can be concluded that the algorithm and the program developed in the present study are reliable.

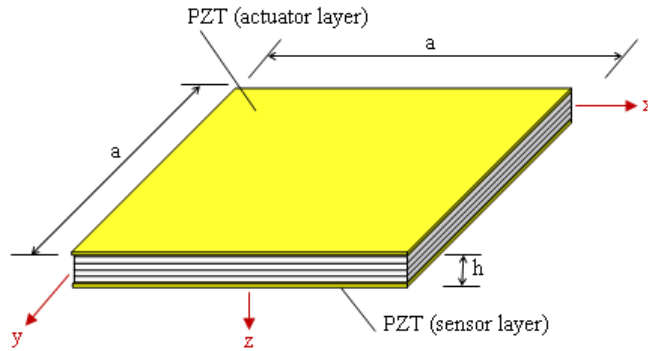


Figure 2. Simply supported piezoelectric sensor/actuator plate.

Table 1. Fundamental frequencies of simply supported six-layer square laminates.

Lay-ups	$\omega_1/100$ in radians per second					
	Closed circuit			Open circuit		
	Akhras [12]	Present	% Error	Akhras [12]	Present	% Error
[p/0°/90°/90°/0°/p]	584.51	577.90	1.14	617.20	601.83	2.55
[p/45°/-45°/45°/-45°/p]	630.80	632.16	0.22	661.39	654.25	1.09
[p/45°/-45°/-45°/45°/p]	635.75	630.23	0.88	666.80	652.90	2.13

5.2. Optimal placement of piezoelectric sensor/actuator pairs on plate using genetic algorithm (GA)

The rectangular plate consisting of four composite layers and two surface-bonded sensor/actuator pairs are now considered. The assumed material properties are the same as problem 5.1. The objective of the optimization problem is to maximize the first natural frequency of the plate with various boundary conditions, geometrical dimensions and lamination sequences. The convergence of genetic algorithm (GA) as shown in Fig. 3.

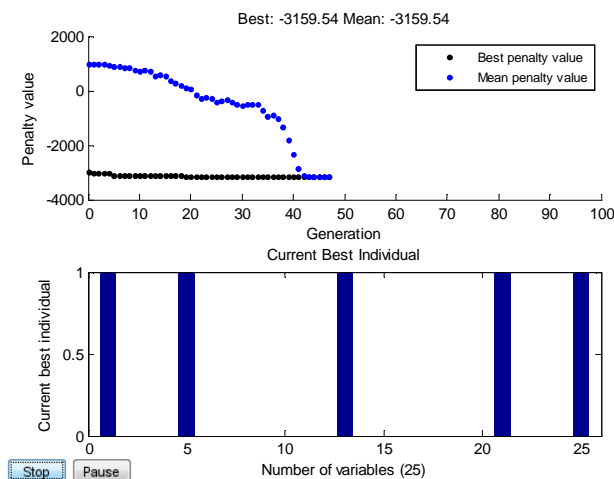


Figure 3. Convergence of GA for SSSS plate.

5.2.1. The effect of boundary conditions

A square plate (0.2×0.2) m with lamination sequence of $[45^\circ/-45^\circ/45^\circ/-45^\circ]$ is studied. Five pairs of piezoelectric sensor/actuator pairs are bonded to each side of the plate (the size of each patch is equal to the size of each element). The plate is under different constraints: SSSS, CCCC, CFCF, CFFF. The results of the optimization problem are summarized in Table 2, and in Figures from 4 to 10.

Table 2. Effect of constraints to optimized deflections.

Case	Boundary condition	Optimized fundamental frequencies ($\omega_1/100$ in rad/s)
1	SSSS	3159.54
2	CCCC	3983.47
3	CFCF	3054.34
4	CFFF	535.34

From the results shown in Table 2 and in Figures from 4 to 7, it is possible to deduce the optimal locations of piezoelectric pairs with respect to different boundary conditions. It is observed that the placement of piezoelectric pairs is optimal when they are closed to the constraints.

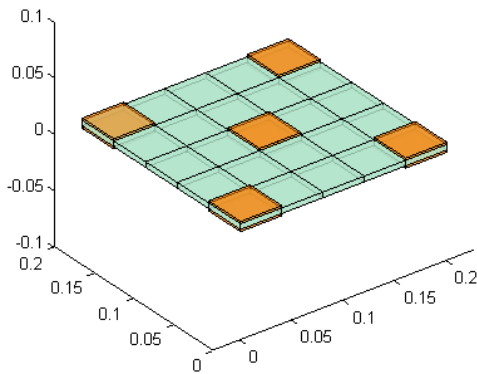


Figure 4. Optimal locations of sensor/actuator on SSSS plate.

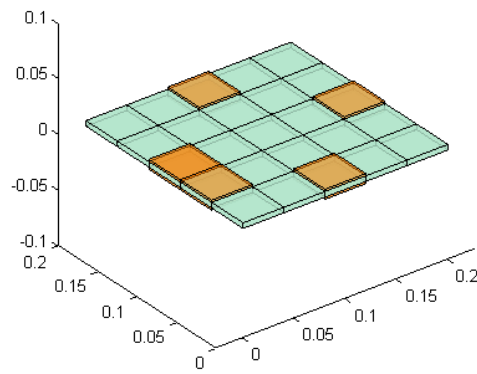


Figure 5. Optimal locations of sensor/actuator on CCCC plate.

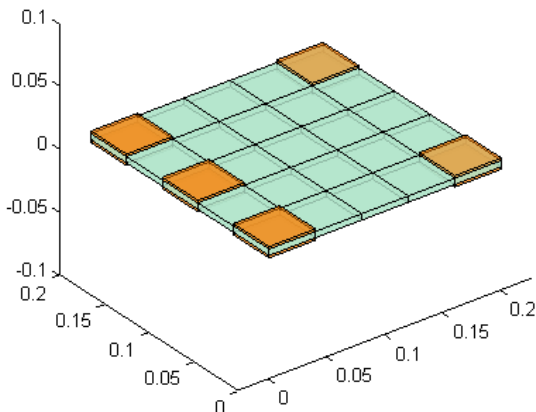


Figure 6. Optimal locations of sensor/actuator on CFCF plate.

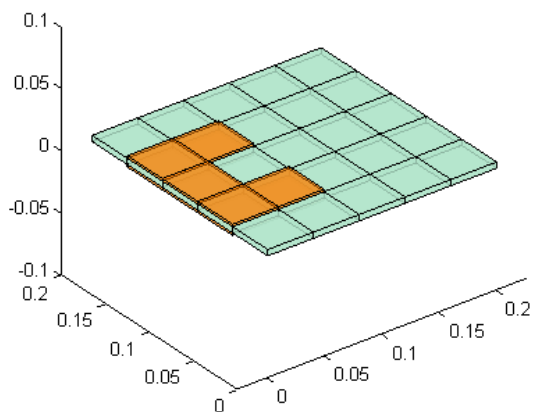


Figure 7. Optimal locations of sensor/actuator on CFFF plate.

5.2.2. The effect of geometrical dimensions of the plate

In this example, two SSSS plates of sizes (0.3×0.2) m and (1×0.2) m with lamination sequence of $[45^\circ/-45^\circ/45^\circ/-45^\circ]$ are studied. Other conditions such as lamination sequence are the same as example 5.2.1 (a). The results of the optimal locations of the patches are shown in Figure 8 and Figure 9.

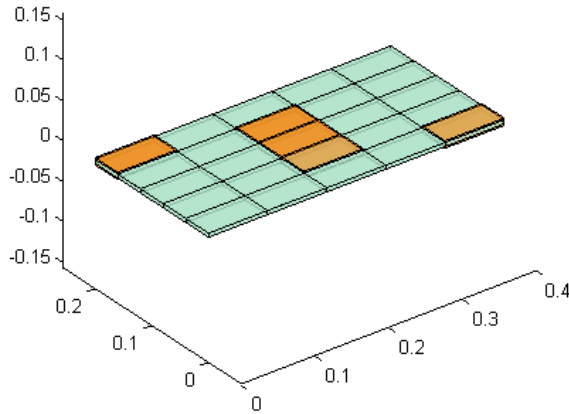


Figure 8. Optimal locations of sensor/actuator on (0.3×0.2) m plate.

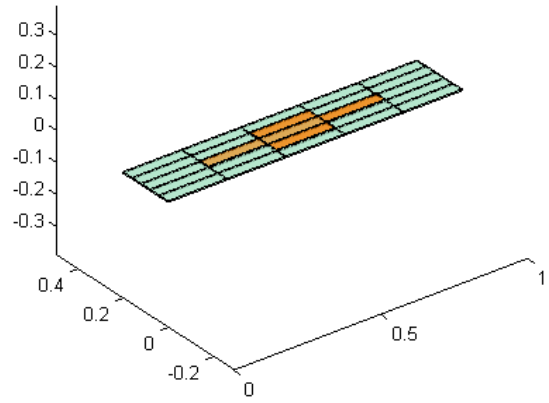


Figure 9. Optimal locations of sensor/actuator on (1.0×0.2) m plate.

The results show that the optimal locations of piezoelectric patches on square plates are different from those on rectangular plates. The optimal locations of piezoelectric patches change as the length-to-width ratio of the rectangular plate changes.

5.2.3. The effect of lamination sequence

In this example, two SSSS square plates (0.2×0.2) m with the following lamination sequences are considered: symmetric $(p/\theta/-\theta/-\theta/\theta/p)$ and anti-symmetric $(p/\theta/-\theta/\theta/-\theta/p)$. The results of optimal locations of piezoelectric patches are shown in Figure 10 and Figure 11.

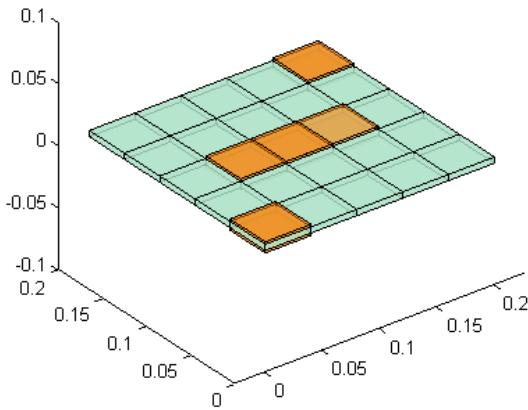


Figure 10. Optimal locations of sensor/actuator in cases of symmetric lamination sequences.

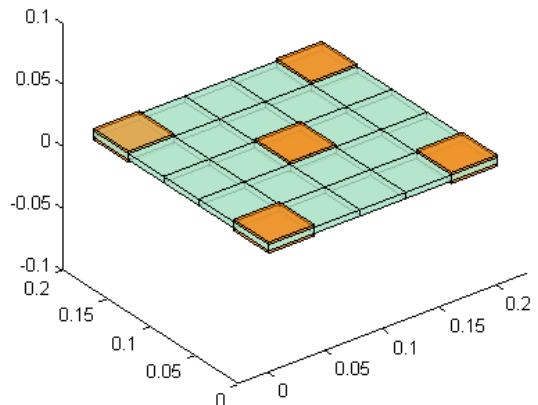


Figure 11. Optimal locations of sensor/actuator in cases of anti-symmetric lamination sequences.

From Figure 10 and Figure 11, it can be observed that optimal locations of piezoelectric patches in case of symmetric lamination sequences are different to those in case of anti-symmetric lamination sequences. In this investigation, in case of symmetric lamination sequences with ply angles of $\theta=45^\circ$ or $\theta=90^\circ$ the optimal locations are symmetric through the diagonal line of the plate as in Figure 10; while in case of anti-symmetric lamination sequences with ply angles of $\theta=45^\circ$ or $\theta=90^\circ$, the optimal locations are rotational symmetric as in Figure 11.

5.2.4. Transient response of composite plates with integrated piezoelectric sensor/actuator pairs

The square plate (0.2×0.2) m with lamination sequence of $[-45^\circ/45^\circ/45^\circ/-45^\circ]$ is considered again to investigate the active vibration control of the cantilever plate. The plate consists of four composite layers and two surface-bonded sensor/actuator patches. The material properties are given in Table 2 following [11]. Here, the dynamic velocity feedback control algorithm is used to actively control the responses of the plate through a closed loop. The Newmark- β method is used to analyze the transient response of the laminated plate. The parameters α and β are selected to be 0.5 and 0.25, respectively. All the simulations of transient response are performed using a time step of 0.01 s.

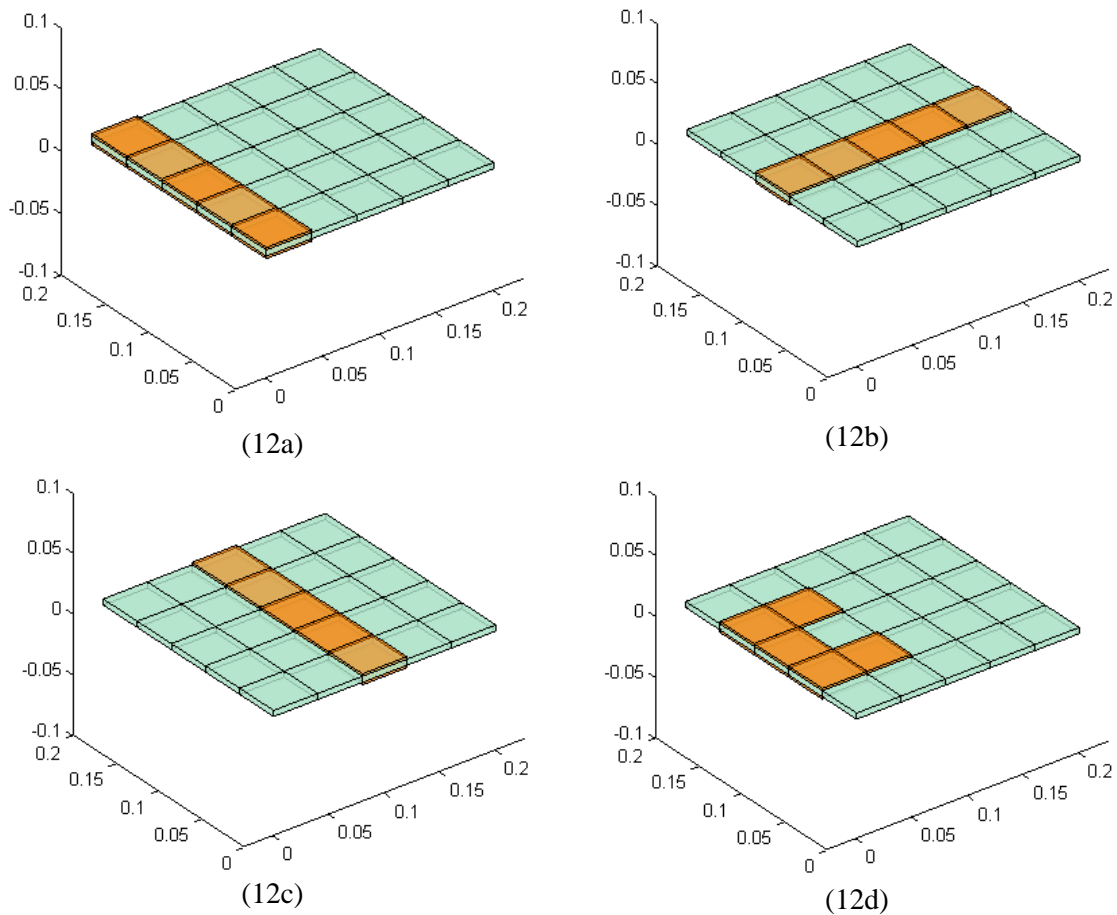
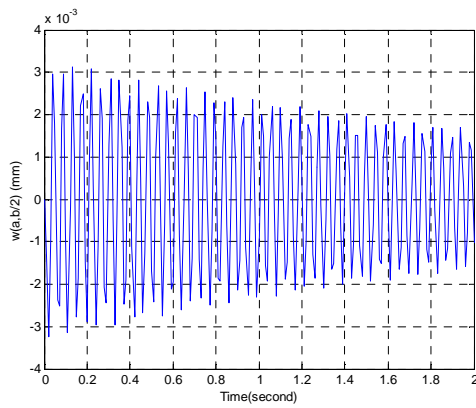


Figure 12. Piezoelectric sensor/actuator pairs configurations.

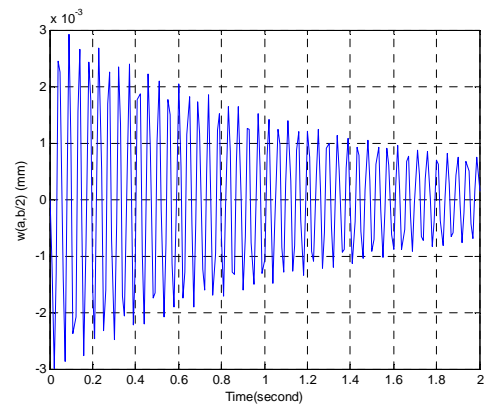
We now consider four cases of placement of piezoelectric patches:

- Case 1: The sensor/actuator piezoelectric pairs are attached close to the clamped-edge – Figure (12a),
- Case 2: The sensor/actuator piezoelectric pairs are attached along the middle line in x -direction – Figure (12b),
- Case 3: The sensor/actuator piezoelectric pairs are attached along the middle line in y -direction – Figure (12c),
- Case 4: Locations of the sensor/actuator piezoelectric pairs are the above-mentioned optimum results in Section 5.2.1 – Figure (12d).

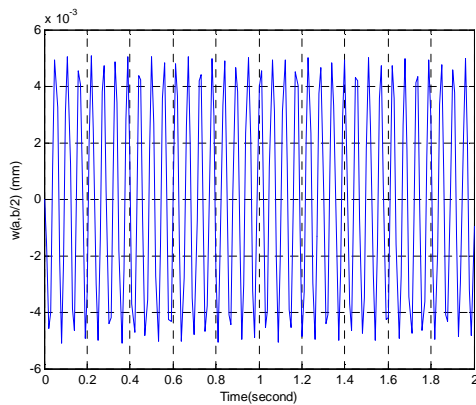
Figures 13 (a-d) show the results of transient analysis of the laminated composite plates integrated sensor/actuator piezoelectric pairs corresponding to the considered cases. The results show that in case 4 (sensor/actuator piezoelectric pairs are similar to reinforcing ribs for plate at the clamped edge), the vibration of the plate damps faster than the others.



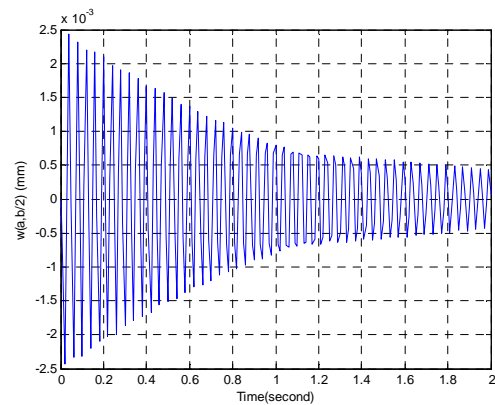
(13a)



(13b)



(13c)



(13d)

Figure 13. Transient response of composite plates with integrated piezoelectric pairs.

6. CONCLUSION

In this study, finite element model based on first-order shear deformation theory is developed and a genetic algorithm is used to formulate the optimization problem. The models are then applied to achieve the optimal design of laminated plates with bonded pairs of sensor/actuator piezoelectric patches. The design objective is the maximization of the fundamental natural frequencies of the plate with various boundary conditions, lamination sequences, and dimensions. The design variables are locations of pairs of piezoelectric patches on the surfaces of the plate.

As shown in the investigated examples, the stiffness of laminated composite plates bonded with sensor/actuator piezoelectric patches can be improved with optimal locations of piezoelectric patches. The results also show that the optimal locations of sensor/actuator piezoelectric patches depend on specific studied cases and the optimal location of sensor/actuator piezoelectric patches not only affects the natural frequency, but also the damping of the vibration of laminated composite plates.

REFERENCES

1. Ning, H. H. - Optimal number & placements of piezoelectric patch actuators in structural active vibration control. *Eng. Comput.* **21** (2004) 651-65.
2. Qiu Z.-C., Zhang X.-M., Wu H.-X., and Zhang H.-H. - Optimal placement and active vibration control for piezoelectric smart flexible cantilever plate. *Journal of Sound and Vibration* **301** (3) (2007) pp. 521-543.
3. Han, J. & Lee, I. - Optimal placement of piezoelectric sensors and actuators for vibration control of a composite plate using genetic algorithms. *Smart Mater. Struct.* **8** (1999) 257-67.
4. Bruant, I., Gallimard, L., & Nikoukar, Sh. - Optimization of Piezoelectric Sensors Location and Number Using a Genetic Algorithm. *Mech. Adv. Mater. Struct* **18** (7) (2001) 469-475.
5. Deepak, C., Gian, B., & Pankaj, C. - Optimal placement of piezoelectric actuators on plate structures for active vibration control via modified control matrix and singular value decomposition approach using modified heuristic genetic algorithm. *Mechanics of advanced materials and structures* **23** (3) (2016) 272-280.
6. Ngoc, L. K., & Thinh, Tr. I. - Optimum problem of piezoelectric laminated composite plate using genetic algorithm. *Vietnam Journal of Mechanics* **31** (1) (2009) 85-105.
7. Cristóvão, M. M., Carlos, A. M & Victor, M. F. - Optimal design of piezolaminated structures. *Composite Structures* **47** (1999) 625-634.
8. Thinh, Tr. I., & Ngoc, L. K. - Static and Dynamic Analysis of Laminated Composite Plates with Integrated Piezoelectrics", *Vietnam Journal of Mechanics* **30** (1) (2008) 55-66.
9. Reddy, J. N. - On laminated composite plates with integrated sensors and actuators. *Engineering Structures* **21** (1999) 568-593.
10. Phung-Van, P., Nguyen-Thoi, T., Le-Dinh, T., & Nguyen-Xuan, H. - Static and free vibration analyses and dynamic control of composite plates integrated with piezoelectric

sensors and actuators by the cell-based smoothed discrete shear gap method (CS-FEM-DSG3). *Smart Mater. Struct.* **22** (2013) 095026 (17pp).

11. Liu G. R., Dai K. Y., & Lim K. M. - Static and vibration control of composite laminates integrated with piezoelectric sensors and actuators using the radial point interpolation method. Institute of Physics Publishing. *Smart Mater. Struct.* **13** (2004) 1438-1447.
12. Akhras, G., & Li, W. - Stability and free vibration analysis of thick piezoelectric composite plates using spline finite strip method. *International Journal of Mechanical Sciences* **53** (2011) 575-584.